



OPEN

Temperature dependence of the thermo-optic coefficient in 4H-SiC and GaN slabs at the wavelength of 1550 nm

Sandro Rao^{1✉}, Elisa D. Mallemace¹, Giuseppe Cocorullo², Giuliana Faggio¹, Giacomo Messina¹ & Francesco G. Della Corte³

The refractive index and its variation with temperature, i.e. the thermo-optic coefficient, are basic optical parameters for all those semiconductors that are used in the fabrication of linear and non-linear opto-electronic devices and systems. Recently, 4H single-crystal silicon carbide (4H-SiC) and gallium nitride (GaN) have emerged as excellent building materials for high power and high-temperature electronics, and wide parallel applications in photonics can be consequently forecasted in the near future, in particular in the infrared telecommunication band of $\lambda = 1500\text{--}1600$ nm. In this paper, the thermo-optic coefficient (dn/dT) is experimentally measured in 4H-SiC and GaN substrates, from room temperature to 480 K, at the wavelength of 1550 nm. Specifically, the substrates, forming natural Fabry–Perot etalons, are exploited within a simple hybrid fiber free-space optical interferometric system to take accurate measurements of the transmitted optical power in the said temperature range. It is found that, for both semiconductors, dn/dT is itself remarkably temperature-dependent, in particular quadratically for GaN and almost linearly for 4H-SiC.

Over the last decade, we seen the rapid development of industrial applications of microelectronic devices based on new semiconducting materials, such as Silicon Carbide (SiC) and Gallium Nitride (GaN). Power electronic applications, in particular, have taken huge advantages from the adoption of these wide bandgap semiconductors, both of which allow the effective fabrication of high breakdown voltage, low on-resistance, diodes and transistors^{1–4}, capable moreover of operating at much higher temperatures compared to Silicon (Si) ones^{5,6}. As the deployment of these materials in electronics is destined to grow in the coming years⁷, it can be expected that this will trigger the development of passive and active photonic devices for communication or sensing purposes, possibly monolithically integrated within the same chip^{8–10}. An obvious prerequisite for the development of such devices is the precise knowledge of the optical properties of these materials, in particular their dependence on temperature variations that can be reached during the operating life.

However, although the temperature dependence of the refractive index is essential for understanding the optical potential of novel materials, such as 4H-SiC and GaN, investigations on the thermo-optic coefficient (TOC) are limited. To date, only a few studies on these wide-bandgap materials can be found in the literature¹¹, based on different experimental methods, such as interferometry¹², z-scan¹³, thermal lens¹⁴ and light-induced transient thermal grating techniques¹⁵, and carried out in various wavelength ranges.

In particular, for the hexagonal (4H) polytype of SiC, although usually regarded among the best materials for high-power electronic and optoelectronic applications¹⁶, an accurate value of the TOC and its temperature dependence is still lacking at the common fiber-optic wavelengths of $\lambda \sim 1.55$ μm .

Scajev et al.¹⁵ applied a time-resolved four-wave mixing technique for the determination of TOCs in heavily doped n-type and p-type 4H-SiC substrates at room temperature (RT). Spatial modulation of thermal properties was achieved by intraband carrier excitation using a light-interference pattern at $\lambda = 1064$ nm and subsequent carrier thermalization. Measurements were carried out in a range of temperature $T = 10\text{--}300$ K, with a calculated value $dn/dT = 3.6 \times 10^{-5} \text{ K}^{-1}$ at $T = 300$ K.

Watanabe et al.¹⁷ investigated the temperature dependence of the refractive indices of 4H-SiC and GaN in a wavelength range from the near band edge ($\lambda = 392$ nm for 4H-SiC, $\lambda = 367$ nm for GaN) to infrared ($\lambda = 1700$ nm)

¹Department DIIES, Mediterranean University, 89124 Reggio Calabria, Italy. ²Department DIMES, University of Calabria, 87036 Cosenza, Italy. ³Department DIETI, University of Naples Federico II, 80125 Naples, Italy. ✉email: sandro.rao@unirc.it

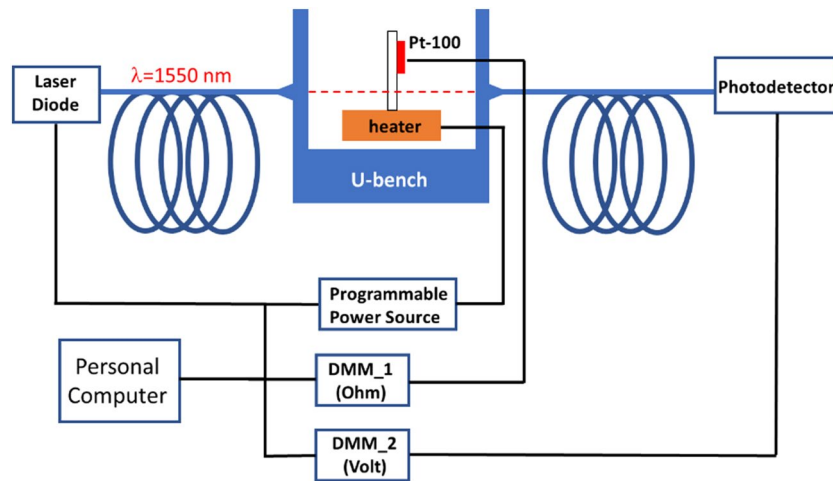


Figure 1. Experimental setup exploited for TOC characterization versus temperature.

from RT to $T = 500$ °C. Optical interference measurements were employed to precisely evaluate ordinary refractive indices. Near the band-edge region, the temperature dependence of the refractive index mainly originates from the temperature change of the bandgap. At $\lambda = 450$ nm, the TOCs of 4H-SiC and GaN were measured to be $7.8 \times 10^{-5} \text{ K}^{-1}$ and $1.6 \times 10^{-4} \text{ K}^{-1}$, respectively.

Xu et al.¹⁸ measured, by the method of minimum deviation, from $T = 293$ K to 493 K, the temperature-dependent refractive indices of 4H- and 6H-SiC over a spectral range from $\lambda = 404.7$ nm to $\lambda = 2325.4$ nm. The TOC dispersion formula as a function of wavelength and temperature was derived from the Sellmeier equation. For 4H-SiC, at the wavelength of $\lambda = 450$ nm, at $T = 493$ K, they calculated a $dn/dT = 8.18 \times 10^{-5} \text{ K}^{-1}$, very close to what was reported in Ref.¹⁷. At the same temperature, for 6H-SiC, the TOC at the wavelength of $\lambda = 1523$ nm is $5.94 \times 10^{-5} \text{ K}^{-1}$, not far from the value of $5.54 \times 10^{-5} \text{ K}^{-1}$ reported in Ref.¹¹.

To our knowledge, to date, there is however a lack of studies in the literature highlighting that the TOC for 4H-SiC and GaN, at $\lambda = 1550$ nm, is itself temperature-dependent, and in a not negligible manner. Therefore, in this letter, we report an experimental characterization of this coefficient for both wide bandgap materials, from RT up to $T = 480$ K, about, at said fiber optic communication wavelength. The results should be helpful for the proper design of 4H-SiC or GaN-based passive and active optoelectronic devices, like waveguides, couplers, interferometers, lasers, switches, modulators, etc. An unknown thermo-optic effect may cause, in fact, incorrect functioning of devices where the temperature dependence of the refractive index is itself temperature and wavelength dependent.

For example, small fluctuations of the TOC with the temperature can lead to significant yet undesirable shifts of resonances in microring-based devices, a phenomenon that is amplified in presence of unavoidable imperfections during the device fabrication processes that result in differences between the dimensions of waveguides, causing an imbalance in the spectral responses to temperature shifts.

Experimental

The samples used in this work are two commercially available¹⁹ semi-insulating thick substrates of 4H-SiC and GaN, both $\langle 001 \rangle$ oriented. The characterization of the thermo-optic coefficient was pursued with the experimental set-up schematically shown in Fig. 1.

In brief, the sample is contained in a U-bench (Thorlabs, FBC-1550-FC) and it is placed on a resistive heater to ensure uniform heating at the desired temperature. The actual temperature of the device under test (DUT) is monitored by a high accuracy PT-100 sensor, firmly glued on it close by the monochromatic light spot. A probe beam at the wavelength of $\lambda = 1.55$ μm , produced by a remotely controlled tunable laser diode, is launched across the sample, orthogonally to the surface. The sample, which is polished at an optical grade on both sides, behaves like a Fabry–Perot (FP) cavity. To calculate the value of dn/dT , the optical tuning and detuning of the FP cavity are monitored with the temperature change. The aim is to measure the temperature variation that is necessary for producing a complete FP detuning, by monitoring the transmitted radiation amplitude collected at the output by an InGaAs, switchable gain, amplified photodetector (Thorlabs, PDA10CS-EC).

For an FP cavity with symmetric mirrors, the transmitted light signal can be calculated by the following expression²⁰:

$$I_t = \frac{I_o}{1 + \frac{4F^2}{\pi^2} \sin^2 \phi} \quad (1)$$

where I_o is the incident light intensity, F is the reflecting finesse of the cavity, and ϕ is the signal phase defined by $\phi = 2\pi nL/\lambda$, with n and L the refractive index and the length of the cavity, respectively.

The sin term confers periodicity to the equation, depending on the variation of the refractive index and on the FP cavity length, which both change with temperature. This trend is explicated by²¹:

	4H-SiC	GaN
Substrate ¹⁹	Semi-insulating <0001>	Semi-insulating (Fe-doped) <0001>
Resistivity ¹⁹	> 10 ⁵ Ω × cm	> 10 ⁶ Ω × cm
Roughness ¹⁹	< 0.5 nm	< 0.5 nm
Energy gap (eV) (T = 300 K)	3.2	3.43
Thickness L (mm) ¹⁹	2	0.35
Thermal expansion coefficient α (10 ⁻⁶ K ⁻¹)	-1.0971 × 10 ⁻⁵ T ² + 1.8967 × 10 ⁻² T - 1.9755 ²⁰	3.92 × 10 ⁻³ T + 2.42 ²³
n (T = 300 K, λ = 1.55 μm)	2.56 ²²	2.32 ^{4,11,23}

Table 1. Main features of the 4H-SiC and GaN samples.

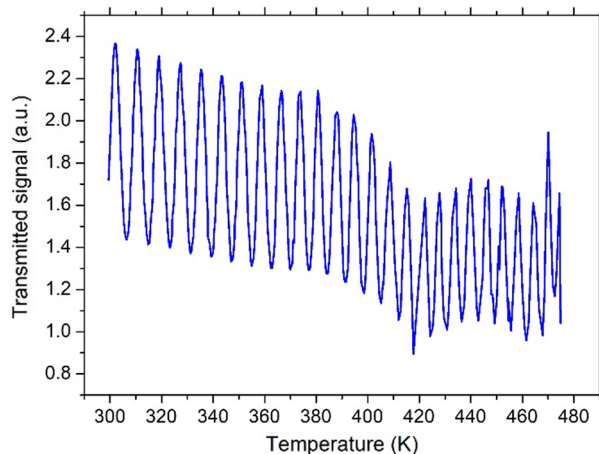


Figure 2. Example of a transmitted signal amplitude plot as a function of temperature for the 4H-SiC sample.

$$\frac{\partial \phi}{\partial T} = \frac{2\pi L}{\lambda} \left(\frac{\partial n}{\partial T} + \alpha(T)n(T) \right) \quad (2)$$

where the term $\alpha = \partial L/L\partial T$ is the thermal expansion coefficient of the semiconducting material.

The temperature dependence of the thermal expansion coefficients for 4H-SiC and GaN are reported in Table 1 together with some specific geometrical parameters.

Results and experimental discussion

Several temperature sweeps were run on each sample. Figure 2 shows an example of the transmitted signal amplitude for the 4H-SiC substrate as a function of temperature from RT to T = 480 K.

The same kind of plots was also obtained from the GaN sample. A sample graph is reported in Fig. 3 in the same range of temperature.

According to (2), the evaluation of the TOC, dn/dT , is obtained from the measurement of the distance in temperature between two consecutive transmission maxima (or minima), ΔT_{π} , corresponding to a phase shift of the optical propagating field of $\Phi = \pi$.

Note that, at each temperature, $\alpha(T)$ is calculated according to the relevant equation in Table 1. In particular, the $\alpha(T)$ dependence for GaN is the linear interpolation of the experimental data provided in Ref. 23, from 300 to 500 K. For what concerns $n(T)$, at each step its value is recursively updated with the value extracted at the previous temperature step.

It is worthwhile specifying that the amplitude drop present in Fig. 2 around 400 K is simply due to a sub-micrometric shift occurred in the mechanical assembly during the several-hours-long automated acquisition. Such events do not affect however the dn/dT extraction, as it only depends on the distance in temperature between consecutive maxima or minima.

Each DUT underwent several temperature ramps, from RT to T = 480 K and, again, from T = 480 K down to RT over a long time (one month). Each temperature sweep required approximately a full day of measurements. Once each operating temperature was reached, the system was kept in a stable condition for about ten minutes before starting the transmitted optical intensity measurement. Five successive and independent acquisitions of the photodetector output signal and the corresponding precise temperatures provided by the PT-100 sensor were subsequently averaged to get a single couple of measurement points, required, instead, only a few seconds. The overall results are summarized in Fig. 4 together with measurements made during the different measurement days.

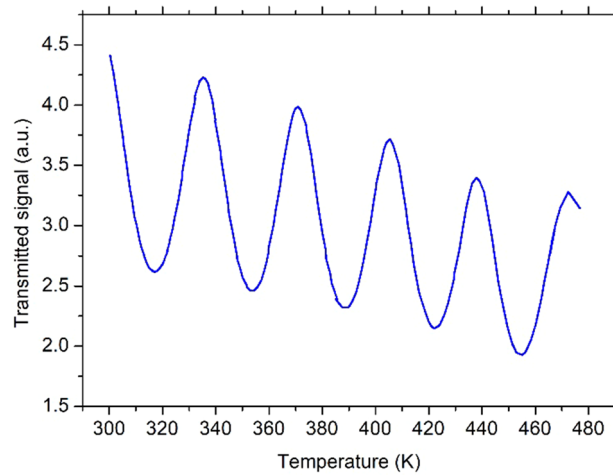


Figure 3. Example of a transmitted signal amplitude plot as a function of temperature for the GaN sample.

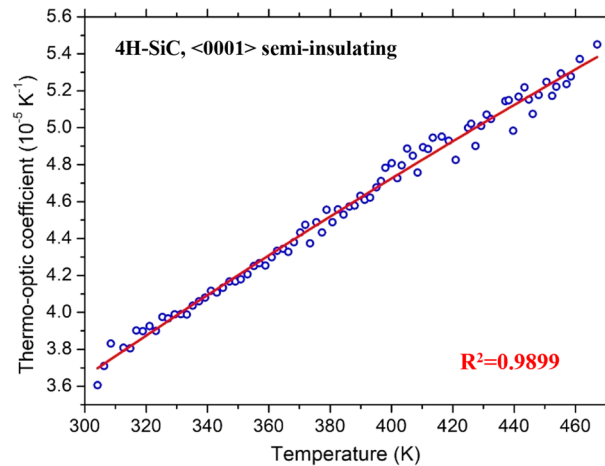


Figure 4. Thermo-optic coefficient as a function of temperature for the 4H-SiC sample.

The same experimental setup was exploited for the characterization of GaN substrate. All of the results are reported in Fig. 5. In this case, the distance in temperature between two consecutive transmission maxima (or minima) is larger with respect to the 4H-SiC substrate due to the reduced thickness of the FP cavity ($L=0.35$ mm), therefore the number of the experimental points of TOC as a function of temperature is limited to only a few values. However, the dependence of the TOC on temperature variation is evident, although less remarkable if compared to the 4H-SiC.

Note that few comparable values of dn/dT are found in the literature for 4H-SiC^{17,18} and GaN^{17,23}, while no temperature dependence has been reported to date.

The experimental data obtained from measurements, at $\lambda = 1550$ nm, were modelled with the 2nd-order polynomial best-fits, $f_L(T)$, described by the following equations:

$$\frac{\partial n}{\partial T} = -5.55 \cdot 10^{-11} T^2 + 1.46 \cdot 10^{-7} T - 2.36 \cdot 10^{-6} \quad \text{for 4H-SiC} \quad (3)$$

$$\frac{\partial n}{\partial T} = -3.81 \cdot 10^{-10} T^2 + 3.45 \cdot 10^{-7} T - 2.07 \cdot 10^{-5} \quad \text{for GaN} \quad (4)$$

The high coefficients of determination (R^2), provided in Figs. 4 and 5, respectively 0.9899 and 0.9699 for 4H-SiC and GaN, demonstrate the good agreement between the experimental points and the polynomial fits. Note that the quadratic coefficient in (3) is very small, suggesting that the TOC dependence for 4H-SiC can be assumed, in fact, linear. Dropping the quadratic dependence leads to the more practical first-order approximation:

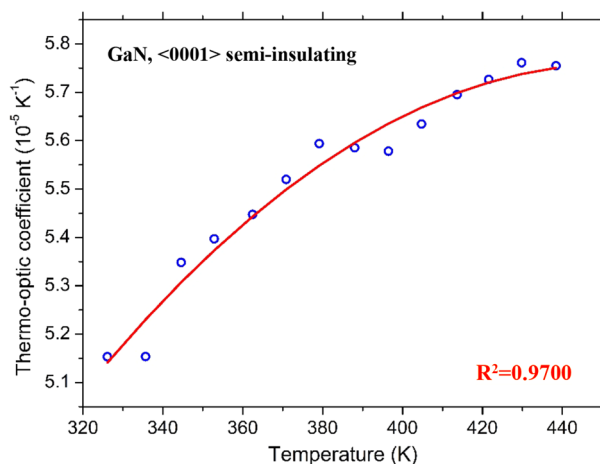


Figure 5. Thermo-optic coefficient as a function of temperature for the GaN sample.

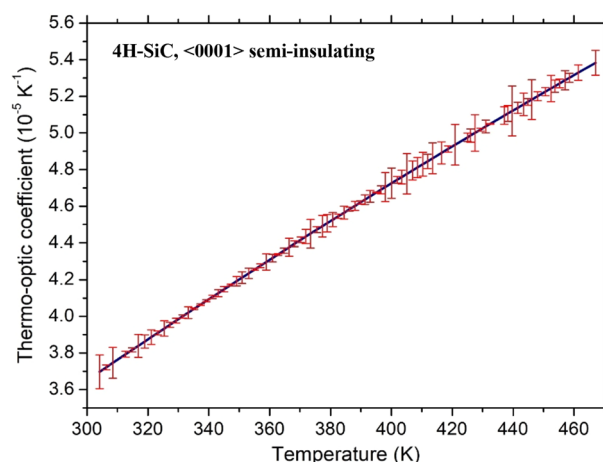


Figure 6. Polynomial fit and error bar of thermo-optic coefficient of 4H-SiC at the wavelength of 1.55 μm .

$$\frac{\partial n}{\partial T} = 1.03 \cdot 10^{-7} T - 5.77 \cdot 10^{-6} \quad \text{for } 4H - \text{SiC} \quad (5)$$

at expenses of a negligible reduction of R^2 , which assumes in this case the value 0.9894.

Another important parameter characterizing the goodness of the calculated TOCs, at the different considered temperatures during all the performed measurements (both positive and negative temperature ramps), with the polynomial best-fit, is the root-mean-square error (*rmse*). In Figs. 6 and 7 the polynomial fit and the relative error bars are reported for both substrates. The corresponding *rmse* values of 4H-SiC and GaN TOCs, in the investigated temperature ranges, are $4.74 \cdot 10^{-7} \text{ K}^{-1}$ and $3.78 \cdot 10^{-7} \text{ K}^{-1}$, respectively, about two orders of magnitude lower with respect to what can be calculated from Eqs. 3 and 4.

Conclusions

In this study, the measurement of the thermo-optic coefficients (dn/dT) and their temperature dependences were reported on 4H-SiC and GaN. The results were accurately evaluated over a wide temperature range from RT to $T = 480 \text{ K}$ at the fiber-optic communication wavelength of $\lambda = 1.55 \mu\text{m}$. The experimental data were modelled with a 2nd-order polynomial best-fit and the coefficient of determination (R^2) and the root mean square error (*rmse*) were calculated. The curves, fitting the TOCs achieved at different temperatures, matches very well the experimental data with a value of R^2 of 0.9899 and 0.9699 for 4H-SiC and GaN, respectively. The TOC increases with temperature for both semiconductors, especially in 4H-SiC where it increases by about 25% for a 100 K temperature variation.

The results can be helpful for the proper design of SiC/GaN-based optoelectronic and nonlinear optical devices, operating in the infrared telecommunication region, that actively use, or are affected by, the refractive index change with temperature.

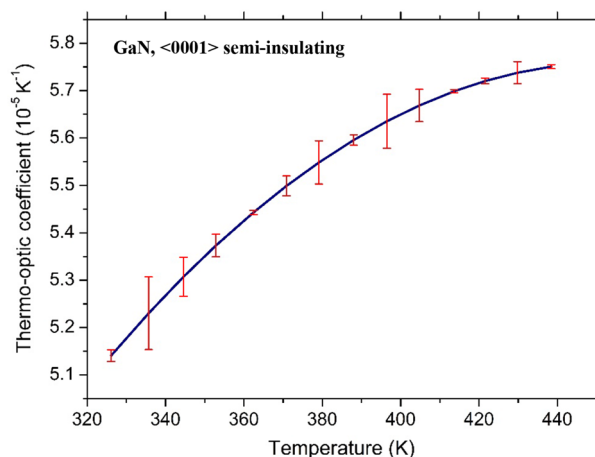


Figure 7. Polynomial fit and error bar of thermo-optic coefficient of GaN at the wavelength of 1.55 μm .

Received: 29 December 2021; Accepted: 2 March 2022

Published online: 21 March 2022

References

- Cooper, J. A. & Agarwal, A. SiC power-switching devices—the second electronics revolution?. *Proc. IEEE* **90**(6), 956–968 (2002).
- Choyke, W. J. *et al.* (eds) *Silicon Carbide: Recent Major Advances* (Springer, New York, 2013).
- Wang, J. & Jiang, X. Review and analysis of SiC MOSFETs' ruggedness and reliability. *IET Power Electron.* **13**(3), 445–455 (2020).
- Oka, T. Recent development of vertical GaN power devices. *Jpn. J. Appl. Phys.* **58**, SB, SB0805 (2019).
- Rabkowski, J., Pefitsis, D. & Nee, H. P. Silicon carbide power transistors: A new era in power electronics is initiated. *IEEE Ind. Electron. Mag.* **6**(2), 17–26 (2012).
- Pearton, S. J. *et al.* GaN electronics for high power, high temperature applications. *Mater. Sci. Eng. B* **82**(1–3), 227–231 (2001).
- Roccaforte, F. *et al.* Emerging trends in wide band gap semiconductors (SiC and GaN) technology for power devices. *Microelectron. Eng.* **187**, 66–77 (2018).
- Monroy, E., Omnès, F. & Calle, F. J. S. S. Wide-bandgap semiconductor ultraviolet photodetectors. *Semicond. Sci. Technol.* **18**(4), R33 (2003).
- Megherbi, M. L. *et al.* An Efficient 4H-SiC photodiode for UV sensing applications. *Electronics* **10**(20), 2517 (2021).
- Della Corte, F. G., Giglio, I., Pangallo, G. & Rao, S. Electro-optical modulation in a 4H-SiC slab induced by carrier depletion in a Schottky diode. *IEEE Photon. Technol. Lett.* **30**(9), 877–880 (2018).
- Della Corte, F. G., Cocorullo, G., Iodice, M. & Rendina, I. Temperature dependence of the thermo-optic coefficient of InP, GaAs, and SiC from room temperature to 600 K at the wavelength of 1.5 μm . *Appl. Phys. Lett.* **77**(11), 1614–1616 (2000).
- Riza, N. A., Arain, M. & Perez, F. 6-H single-crystal silicon carbide thermo-optic coefficient measurements for ultrahigh temperatures up to 1273 K in the telecommunications infrared band. *J. Appl. Phys.* **98**(10), 103512 (2005).
- De Nalda, R. *et al.* Limits to the determination of the nonlinear refractive index by the Z-scan method. *JOSA B* **19**(2), 289–296 (2002).
- Anjos, V. *et al.* Thermal-lens and photo-acoustic methods for the determination of SiC thermal properties. *Microelectron. J.* **36**(11), 977–980 (2005).
- Ščajev, P. & Jarašiūnas, K. Application of a time-resolved four-wave mixing technique for the determination of thermal properties of 4H-SiC crystals. *J. Phys. D Appl. Phys.* **42**(5), 055413 (2009).
- Zhao, F., Islam, M. M., Muzykov, P., Bolotnikov, A. & Sudarshan, T. S. Optically activated 4H-SiC pin diodes for high-power applications. *IEEE Electron Device Lett.* **30**(11), 1182–1184 (2009).
- Watanabe, N., Kimoto, T. & Suda, J. Thermo-optic coefficients of 4H-SiC, GaN, and AlN for ultraviolet to infrared regions up to 500 C. *Jpn. J. Appl. Phys.* **51**(11R), 112101 (2012).
- Xu, C. *et al.* Temperature dependence of refractive indices for 4H- and 6H-SiC. *J. Appl. Phys.* **115**(11), 113501 (2014).
- http://www.crystal-material.com/Substrate-Materials/list_44_1.html.
- Born, M. & Wolf, E. *Principles of Optics* (Pergamon Press, Oxford, UK, 1989).
- Cocorullo, G., Della Corte, F. G. & Rendina, I. Temperature dependence of the thermo-optic coefficient in crystalline silicon between room temperature and 550 K at the wavelength of 1523 nm. *Appl. Phys. Lett.* **74**, 3338 (1999).
- Nakabayashi, M., Fujimoto, T., Katsuno, M., & Ohtani, N. Precise determination of thermal expansion coefficients observed in 4H-SiC single crystals. In *Materials Science Forum*, Vol. 527, 699–702 (2006).
- Reeber, R. R. & Wang, K. Lattice parameters and thermal expansion of GaN. *J. Mater. Res.* **15**(1), 40–44 (2020).

Author contributions

S.R., G.C., and F.G.D.C. conceived the experiments and the methodology. S.R., E.D.M., G.F. and F.G.D.C. conducted the experiments and performed the statistical analysis and figure generation. Supervision: S.R., G.M. and F.G.D.C. All authors reviewed the manuscript.

Competing interests

The authors declare no competing interests.

Additional information

Correspondence and requests for materials should be addressed to S.R.

Reprints and permissions information is available at www.nature.com/reprints.

Publisher's note Springer Nature remains neutral with regard to jurisdictional claims in published maps and institutional affiliations.



Open Access This article is licensed under a Creative Commons Attribution 4.0 International License, which permits use, sharing, adaptation, distribution and reproduction in any medium or format, as long as you give appropriate credit to the original author(s) and the source, provide a link to the Creative Commons licence, and indicate if changes were made. The images or other third party material in this article are included in the article's Creative Commons licence, unless indicated otherwise in a credit line to the material. If material is not included in the article's Creative Commons licence and your intended use is not permitted by statutory regulation or exceeds the permitted use, you will need to obtain permission directly from the copyright holder. To view a copy of this licence, visit <http://creativecommons.org/licenses/by/4.0/>.

© The Author(s) 2022